



## Biosorption of bioactive compounds in bacterial nanocellulose: Mechanisms and physical-chemical properties

Isabela de Andrade Arruda Fernandes<sup>a</sup>, Giselle Maria Maciel<sup>b</sup>, Isabela Sampaio Ribeiro<sup>a</sup>,  
Alessandra Cristina Pedro<sup>a</sup>, Débora Gonçalves Bortolini<sup>a</sup>, Valéria Rampazzo Ribeiro<sup>a</sup>,  
Lillian Barros<sup>c,d</sup>, Charles Windson Isidoro Haminiuk<sup>b,\*</sup>

<sup>a</sup> Programa de Pós-Graduação em Engenharia de Alimentos (PPGEAL), Universidade Federal do Paraná (UFPR), 81531-980 Curitiba, Paraná, Brazil

<sup>b</sup> Laboratório de Biotecnologia, Universidade Tecnológica Federal do Paraná (UTFPR), 81280-340 Curitiba, Paraná, Brazil

<sup>c</sup> Centro de Investigação de Montanha (CIMO), Instituto Politécnico de Bragança, Campus de Santa Apolonia, 5300-253 Bragança, Portugal

<sup>d</sup> Laboratório Associado para a Sustentabilidade e Tecnologia em Regiões de Montanha (SusTEC), Instituto Politécnico de Bragança, Campus de Santa Apolonia, 5300-253 Bragança, Portugal

### ARTICLE INFO

#### Keywords:

Biopolymers  
Bioactive compounds  
Biosorption  
Antioxidants  
Recovery of food residue

### ABSTRACT

Bacterial cellulose (BC) is a biomaterial produced by *Gluconacetobacter xylinus*, with wide applicability in different areas, such as biomedical, pharmaceutical, and food. BC production is usually carried out in a medium containing phenolic compounds (PC), such as teas, however, the purification process leads to the loss of such bioactive. Thus, the innovation of this research consists of the reincorporation of PC after the purification of the BC matrices through the biosorption process. In this context, the effects of the biosorption process in BC were evaluated to maximize the incorporation of phenolic compounds from a ternary mixture of hibiscus (*Hibiscus sabdariffa*), white tea (*Camellia sinensis*), and grape pomace (*Vitis labrusca*). The biosorbed membrane (BC-Bio) showed a great concentration of total phenolic compounds (TPC = 64.89 mg L<sup>-1</sup>) and high antioxidant capacity through different assays (FRAP: 130.7 mg L<sup>-1</sup>, DPPH: 83.4 mg L<sup>-1</sup>, ABTS: 158.6 mg L<sup>-1</sup>, TBARS: 234.2 mg L<sup>-1</sup>). The physical tests also indicated that the biosorbed membrane presented high water absorption capacity, thermal stability, low permeability to water vapor and improved mechanical properties compared to BC-control. These results indicated that the biosorption of phenolic compounds in BC efficiently increases bioactive content and improves physical membrane characteristics. Also, PC release in a buffered solution suggests that BC-Bio can be used as a polyphenol delivery system. Therefore, BC-Bio is a polymer with wide application in different industrial segments.

### 1. Introduction

Bacterial cellulose (BC) is a biopolymer with easy production and high performance that has been used in the biotechnological area due to its unique properties, such as thermal stability, purity and compatibility [1]. In addition to these properties, BC has nanostructures that allow a high capacity of absorption of water and nanocomposites [2], promoting the membrane antioxidant capacity by incorporating compounds such as anthocyanins [3], tannin acid [4], wine residues [5] and plant extract [6,7]. Thus, BC is an excellent bioactive delivery system, which can be optimized through processes that aim at the maximum incorporation of bioactive molecules [8], such as biosorption.

Biosorption is a process used to describe the accumulation and

removal of elements of aqueous solutions by physical-chemical interactions with the cellular components of biological materials such as algae, bacteria, fungi, yeasts [9] and by-products [10,11]. This mechanism can cover processes of surface adsorption and sequestration of microstructures, electrostatic attraction, complexation, covalent forces, van der Waal forces and/or ion exchange [12]. In addition, this technique has been proposed for the bioactivity of phenolic compounds (PC) that depend on their cellular purpose and physical characteristics [13].

Generally, PC is divided into phenolic acids, stilbenes, flavonoids and lignans, which can be extracted from plants, such as using tea leaf infusion techniques [14,15]. Phenolic compound surfaces have bioactivity limited absorption and transport efficiency to achieve biopolymer structures. Thus, the enrichment of biological matrices (biosorbent) with

\* Corresponding author.

E-mail address: [haminiuk@utfpr.edu.br](mailto:haminiuk@utfpr.edu.br) (C.W.I. Haminiuk).

<https://doi.org/10.1016/j.ijbiomac.2023.124349>

Received 6 December 2022; Received in revised form 14 March 2023; Accepted 3 April 2023

Available online 11 April 2023

0141-8130/© 2023 Elsevier B.V. All rights reserved.

PC through biosorption is a new approach that can be explored. PC are secondary metabolites that, in addition to having antioxidant properties important for technological applications, have importance in maintaining human health, such as antitumor, cardiac and gastrointestinal protection, as well as anti-inflammatory and antimicrobial properties [16–18]. This technology has successfully been tested for the biosorption of phenolic compounds from teas and grape pomace [19]. However, the novelty of this work is the addition of hibiscus flower extracts, aiming modify phenolic characteristic of BC membrane.

Among the plants of *Camellia sinensis*, white tea has a delicate process that conserves the high content of phenolic compounds derived from flavonoids in its composition [18,19]. Thus, white tea has a high antioxidant activity responsible for making it more attractive for consumption [20,21]. Due to its phytochemical constitution, the hibiscus plant also has aroused interest in nutritional, industrial and medicinal applications. Its extract has organic acids (ascorbic acid, citric acid, maleic acid and tartaric acid), phenolic compounds, anthocyanins and other water-soluble antioxidants [22]. In addition, hibiscus is effective against hypertension, inflammation, liver disorders, diabetes and metabolic syndrome [23]. Furthermore, by-products derived from the wine industry, such as grape pomace, can be considered a valuable source of natural phytochemicals, including phenolic compounds and other bioactive compounds that can be used as functional compounds in the pharmaceutical, cosmetic and food sectors [24].

The objective of this research was to evaluate the biosorptive potential of phenolic compounds of a ternary mixture (white tea, hibiscus, and grape pomace) in bacterial cellulose. For this, different isotherm models were applied in order to clarify the biosorption mechanism. In addition, the biosorbed membrane was characterized in relation to its chemical and mechanical properties in order to evaluate the effects of phenolic biosorption on the membrane. The different membrane characterization assays performed before and after biosorption have the purpose of identifying possible changes in membrane characteristics with the insertion of total phenolic compounds.

## 2. Materials and methods

### 2.1. Reagents and standards

Reagents (analytical grade) and standards (HPLC grade) were purchased from Synth (Diadema, SP, Brazil), Dynamics (Indaiatuba, SP, Brazil), and Sigma-Aldrich (São Paulo, SP, Brazil).

### 2.2. Raw material

The culture *Gluconacetobacter xylinus* (ATCC 10245 registered in the National System of Management of Genetic Heritage and Associated Traditional Knowledge (SisGen - A7E5B69), used for the production of cellulose, was obtained from the Laboratório de Biotecnologia (Labiotec group) of the Universidade Federal do Paraná (UTFPR, Curitiba, Brazil). Sucrose, white tea (*Camellia sinensis*) and hibiscus flowers (*Hibiscus sabdariffa*) were purchased at the Municipal Market of Curitiba, Paraná, Brazil. In addition, grape pomace, composed of peel, seed and stem of *Vitis labrusca* species, was obtained from Toledo, PR, Brazil, as a by-product of the wine-making process. The grape pomace varieties were subjected to the drying process in an air circulation oven at 40 °C, ground in a knife mill and stored under refrigeration at –20 °C, until the moment of the analyses.

### 2.3. Biosorbent preparation

The BC membrane was produced in an optimized culture medium, according to the methodology of Fernandes et al. [19], this medium was chosen because it results in a high production of bacterial cellulose in a shorter time. First, the inoculum was obtained by incubation of 15 g of mother bacterial cellulose in Hestrin-Schramm [25] culture medium for

ten days at 28 °C. After the formation of a new membrane, it was cut into disks (diameter and thickness of 2.2 and 1.0 mm, respectively) and used in the present experiment. The medium was composed of autoclaved-distilled water (1 L), sucrose (70 g L<sup>-1</sup>), 95 % ethanol (30 mL L<sup>-1</sup>), acetic acid (5 mL L<sup>-1</sup>), white tea (1.98 g L<sup>-1</sup>), hibiscus (0.51 g L<sup>-1</sup>), grape pomace (0.51 g L<sup>-1</sup>) and 500 mg L<sup>-1</sup> of Centrum® vitamin complex (Composition: vitamin A, vitamin D, vitamin C, vitamin E, vitamin B1, vitamin B2, vitamin B3, biotin, pantothenic acid, vitamin K, calcium, iron, magnesium, zinc, iodine, copper, selenium, molybdenum, chromium, manganese and phosphorus). In a rectangular container (16.5 × 11.5 × 6 cm), two disks (diameter and thickness of 2.2 and 1.0 mm, respectively) of BC (inoculum) were added to 150 mL of culture medium and incubated statically at 28 °C for seven days. After incubation, BC membranes were purified with NaOH 0.1 mol L<sup>-1</sup> solution at 80 °C for 2 h, this purification eliminates both microbial load and totally degrades phenolic compounds that could be present in the membrane. Subsequently, the membrane was washed with distilled water [26] and frozen (–18 °C) in 20 % glycerol solution until the moment of analysis. Glycerol acts as cryoprotector of the BC membrane, preventing ice crystals from drilling the membrane during thawing.

### 2.4. Preparation of extract for biosorption

The extract of the ternary mixture (66 % white tea, 17 % Hibiscus, and 17 % grape pomace, m/v) was prepared from its infusion, where 1 g of the ternary mixture (0.66 g white tea, 0.17 g hibiscus, and 0.17 g grape pomace) was placed in a sachet infuser (material: cellulose, origin: Japan, brand: Komoda, dimension: 9.5 × 7 cm) and immersed in 100 mL of ultrapure water at 90 °C, under the ultrasonic bath (SolidSteel, SSBu 3.8 L, frequency of 40 KHz and power of 100 W) for 15 min. These conditions were applied according to the results obtained from the simplex-centroid methodology studied by Fernandes et al. [19]. In this study a high concentration of phenolic compounds and high antioxidants values were obtained for ternary mixture; thus, we choose the same conditions for the biosorption tests. In addition, it is known that the interaction between phenolics and the membrane depends on the molecular weight of the compounds [27], and it is important to have a diversification of them.

### 2.5. Preparation of biosorbed bacterial cellulose membrane

The kinetics study for incorporating phenolic compounds in BC followed the method proposed by Ribeiro et al. [28] with some modifications. In Erlenmeyer bottles of 50 mL, 630 ± 10 mg of bacterial cellulose membrane (wet weight), and 15 mL of ternary mixture extract solution (66 % white tea, 17 % Hibiscus, and 17 % *Vitis labrusca* grape pomace) were added. The Erlenmeyers were placed under an ultrasonic bath at 25 °C, and the samples were taken at intervals of 10, 20, 30, 60, 120, and 240 min to analyze the concentration of total phenolic compounds (TPC) in solution. Control samples of each point (considering time and extract sample) were performed to remove possible interferences. The concentration of adsorbed TPC (qt) in mg g<sup>-1</sup> was determined by mass balance according to Eq. (1) (Table 1).

The same conditions as the kinetic study were performed for adsorption isotherm assays. However, the concentration of the extract was varied in 4 dilutions (2, 4, 6, and 8 mg L<sup>-1</sup>) from the mother solution (ternary mixture) of 10 g L<sup>-1</sup>, using the equilibrium time of 120 min found in the kinetic test, which is the time that presents the highest concentration of TPC adsorbed (Supplementary Material: Table S1). The mathematical models of three Hill and Sips parameters were used to describe and evaluate the behavior of the adsorption process of the total phenolic compounds BC membrane (Table 1). The models were adjusted in non-linear form using Origin 7.0 software (OriginLab, Northampton, MA) [29,30].

**Table 1**

Models and equations used to calculate isothermal parameters.

Models	Equation	n.
Mass Balance	$q_t = \frac{(C_0 - C_t)V}{m}$	(1)
Isothermal models		
Hills	$q_e = \frac{q_{\max} C_e^{n_H}}{K_H + C_e^{n_H}}$	(2)
Sips	$q_e = \frac{q_{\max} K_S C_e^S}{1 + K_S C_e^S}$	(3)

Note:  $q_t$ : the biosorption capacity ( $\text{mg g}^{-1}$ ) in time  $t$  (min),  $C_0$  e  $C_t$ : the concentrations of total phenolic compounds before and after biosorption in time  $t$  ( $\text{mg L}^{-1}$ ), respectively,  $V$ : the volume of aqueous phase (L),  $m$ : BC membrane mass (g);  $q_e$ : sorption capability in balance ( $\text{mg g}^{-1}$ ),  $q_{\max}$ : maximum adsorption capacity ( $\text{mg g}^{-1}$ );  $C_e$ : concentration of the solution in balance ( $\text{mg L}^{-1}$ ),  $K_H$ : ( $\text{L mg}^{-1}$ ), and  $n_H$ : constants of the Hills model,  $K_S$ : Sips adsorption constant,  $S$ : empirical constant of Sips.

## 2.6. Membrane preparation for TPC determination and antioxidant activity

The control bacterial cellulose membrane (BC-Control) and biosorbed bacterial cellulose membrane (BC-Bio) were cut into  $1 \text{ cm}^2$  (100 mg) and immersed in 2 mL of methanol for 24 h at room temperature, this technique was followed according to the protocol developed by Yang et al. [31] because it is a simple technique that confers less error. Subsequently, the solvent was used to determine TPC and antioxidant activity [31].

## 2.7. Determination of total phenolic compounds (TPC)

The quantification of TPC was performed according to the colorimetric method of Folin-Ciocalteu, described by Singleton & Rossi [32] and Ribeiro et al. [28]. First, the extract of the samples (100  $\mu\text{L}$ ) was mixed with 5150  $\mu\text{L}$  of ultrapure water and then 350  $\mu\text{L}$  of the Folin-Ciocalteu reagent was added and incubated in the dark for 3 min at  $25^\circ\text{C}$ . Then, 1400  $\mu\text{L}$  of 20 % sodium carbonate was added to the mixture that remained incubated in the dark for 2 h. The readings were performed with a spectrophotometer (UV M51, BEL Engineering) at 765 nm. A calibration curve of gallic acid was determined ( $y = 0.0015x - 0.0169$ ,  $R^2 = 0.9937$ ) and the results were expressed in equivalent milligram of gallic acid per liter of extract ( $\text{mg GAE L}^{-1}$ ).

## 2.8. Antioxidant capacity of the samples

### 2.8.1. DPPH method

The determination of antioxidant activity in extracts by the DPPH method was according to Brand-Williams et al. [33] with some modifications. First, 1180  $\mu\text{L}$  of ethanol, 1070  $\mu\text{L}$  of DPPH solution and 250  $\mu\text{L}$  of extract were mixed and kept in the dark for 30 min. The readings were performed in a spectrophotometer at 517 nm. The Trolox calibration curve was constructed ( $y = -0.0017x + 0.9637$ ,  $R^2 = 0.9801$ ) and the results were expressed in  $\mu\text{mol}$  of Trolox equivalent per liter of extract ( $\mu\text{molTE L}^{-1}$ ).

### 2.8.2. ABTS method

The determination of the inhibition activity of the ABTS radical was performed according to Re et al. [34] with some modifications. First, 4 mL of ABTS radical solution (ABTS and potassium persulfate) was added to 40  $\mu\text{L}$  of the extracts. At room temperature, the mixture rested in the dark for 6 min. Then, a spectrophotometer was read at 734 nm. The antioxidant capacity of the extracts was presented as  $\mu\text{mol}$  value of equivalent Trolox per liter of extract ( $\mu\text{molTE L}^{-1}$ ) from a standard curve of Trolox ( $y = -0.0002x + 0.6729$ ,  $R^2 = 0.9776$ ).

## 2.8.3. FRAP method

The fluorescence recovery after the photobleaching (FRAP) trial was made according to the methodology of Benzie & Strain [35]. The tubes containing samples and FRAP reagent (TPTZ, sodium acetate buffer, and  $\text{FeCl}_3$ ) were stirred and incubated for 30 min in a water bath with water circulation (LT202/30, LimaTec) at  $37^\circ\text{C} \pm 1$  and absorbance was determined in a spectrophotometer at 594 nm. The reducing potential was expressed in units of mmol of Trolox equivalent per liter of extract ( $\mu\text{molTE L}^{-1}$ ) from a standard curve of Trolox ( $y = 0.0023x + 0.0472$ ,  $R^2 = 0.9956$ ).

## 2.8.4. TBARS method

TBARS assay is based on inhibiting lipid peroxidation using thiobarbituric acid (TBARS) reactive substances. For this method, pig brains (*Sus scrofa*) were obtained from official slaughter animals, dissected, and homogenized with a Polytron in frozen tris-HCl buffer (20 mM, pH 7.4). Then, this mixture was centrifuged at 3000  $\times g$  for 10 min to produce a homogenized 1:2 (w/v) brain tissue. Next, an aliquot (0.1 mL) of the supernatant was incubated with different concentrations of phenolic extract solution (0.2 mL) in the presence of  $\text{FeSO}_4$  (10  $\mu\text{M}$ ; 0.1 mL) and ascorbic acid (0.1 mM; 0.1 mL) at  $37^\circ\text{C}$  for 1 h. The reaction was interrupted by adding trichloroacetic acid (28 % w/v, 0.5 mL), followed by thiobarbituric acid (TBA, 2 %, w/v, 0.38 mL) and the mixture was then heated to  $80^\circ\text{C}$  for 20 min. Subsequently, the solution was centrifuged at 3000  $\times g$  for 10 min to remove the precipitated protein. The color intensity of the malondialdehyde complex (MDA)-TBA in the supernatant was measured by absorption at 532 nm [36].

## 2.9. Identification and quantification of bioactive compounds by HPLC-DAD/UV-vis

Bioactive compounds were identified and quantified by high-performance liquid chromatography coupled with diode array detection (HPLC-DAD, Prominence Model, Shimadzu). The samples were previously filtered through a filter with pores of 0.22  $\mu\text{m}$  and the Hypersil BDS column (C18, 250  $\times$  6 mm) was used for the separation of the compounds. The analysis was performed using two different methods to obtain better separation of the compounds.

### 2.9.1. Method 1

The mobile phase consisted of acetonitrile (A) and water acidified with 0.1 % acetic acid (B). The gradient was described as follows: Up to 10 min 5 % A; 10 to 50 min 95 % A; from 50 to 55 min 5 % A, maintained until 60 min for stabilization. The injection volume was 10  $\mu\text{L}$  and the flow rate was 1  $\text{mL min}^{-1}$ . The analysis was performed at  $35^\circ\text{C}$  and the run time was 60 min. This method separated some phenolic acids such as gallic acid, chlorogenic acid, vanillic acid, caffeic acid, syringic acid, p-coumaric acid, ferulic acid and two flavonoids, epicatechin and naringin.

### 2.9.2. Method 2

This method separated flavonoids, for example, catechin, procyanidin B2 and cyanidin-3-O-glucoside. The run time was 45 min. The mobile phase comprised Acetonitrile (B), methanol (C) and water acidified with 0.1 % phosphoric acid. The gradient started with 3 % B + 2 % C, 3 % B + 5 % C up to 5 min, 5 % B + 15 % C up to 10 min, 5 % B + 25 % C up to 25 min, 30 % B + 30 % C up to 30 min, between 35 and 45 min the column was stabilized for the initial conditions. The injection volume was 10  $\mu\text{L}$  and the flow rate was 1  $\text{mL min}^{-1}$ . The analysis was performed at  $30^\circ\text{C}$  and the run time was 45 min. For both methods, the detection was performed with a diode array according to the parameters described in Table 2.

## 2.10. Characterization of the membrane by MIR-ATR

The chemical structure of the control and biosorbed membranes was

**Table 2**  
Identification and quantification parameters of phenolic compounds.

Compound	a	b	R <sup>2</sup>	RT (min)	λ (nm)	LOQ (mg L <sup>-1</sup> )	LOD (mg L <sup>-1</sup> )
Caffeic acid	33,016.61	-593.60	0.9999	20.89	323	0.18	0.06
Catechin	6302.04	-61.87	0.9998	17.95	280	0.52	0.03
Chlorogenic acid	23,935.04	-1105.17	0.9998	19.35	326	0.46	0.15
Cyanidin-3-O-glucoside	21,910.68	-1296.05	0.9989	24.47	516	0.45	0.20
Epicatechin	37,825.28	-739.28	0.9998	21.24	275	0.20	0.06
Ferulic acid	27,738.96	-665.49	0.9999	24.33	322	0.24	0.08
Gallic acid	14,193.51	-2023.73	0.9988	6.12	271	1.43	0.47
Naringin	23,061.67	581.94	0.9998	24.7	283	0.25	0.08
p-coumaric acid	33,114.08	-884.38	0.9998	23.4	309	0.27	0.09
Procyanidin B2	4565.06	-197.24	0.9986	19.34	280	0.47	0.14
Syringic acid	17,859.86	58.33	0.9998	23.81	295	0.03	0.01
Vanillic acid	31,807.32	-123.75	0.9998	20.63	261	0.04	0.01

Note: a: Angular coefficient of the calibration line. b: Linear coefficient of the calibration line. R<sup>2</sup>: Coefficient of determination of the line. RT: Retention time. λ: Identification wavelength. LOQ: Limit of quantification. LOD: Limit of detection.

characterized using mid-infrared spectroscopy with attenuated total reflection (MIR-ATR) using the spectrometer (Varian, 640-IR, California, USA). The scans were performed at wavelengths 500 to 4000 cm<sup>-1</sup> [37].

### 2.11. Evaluation of the membrane topography by MEV and AFM

The control and biosorbed membranes were coated with 90 nm of gold in preparation for scanning electron microscopy (SEM) images (Quanta 450 FEG, FEI and Vega3, Tescan), operating at 15 kV and with a magnification of 20,000–75,000 times [38]. Amplifications are different between membranes, since they were adjusted according to the clear visualization of membrane structures, thus observing whether there were changes in structures and topographies. Atomic force microscopy (AFM) images were used to determine the surface of the membranes, which were acquired in dynamic mode in an atomic force microscope (SPM-9700 HT, Shimadzu). The NCHR (BudgetSensors) tip was used with a force constant of 40 N m<sup>-1</sup> and a resonance frequency of 300 kHz. The scanning area was 2–3 × 2–3 μm<sup>2</sup>, scan speed 0.8 Hz, resolution of 512 × 512 pixels and operating point of ~0.2 V.

### 2.12. Thermal stability analysis

The thermogravimetric analyzer determined the mass variation of the membranes along with temperature variation and their thermal stability (TGA 4000, Perkin Elmer). Thermal analyses are standard techniques and are required for knowledge of the thermal behavior of a biopolymer. It is noteworthy that temperature determines the thermodynamic behavior of biopolymers and is therefore important to direct its applications [39]. Thus, approximately 8 mg of the samples were packed in hermetically sealed aluminum cells under heating from 30 to 600 °C with a heating rate of 10 °C min<sup>-1</sup> using a nitrogen atmosphere whose flow was 50 mL min<sup>-1</sup>.

### 2.13. Water absorption capacity

The water absorption capacity (WAC) was evaluated by immersion the control and biosorbed membranes in deionized water and storing until equilibrium (approximately 48 h) in an oven at 35 °C ± 2. Then, the surface water of the membrane (control and biosorbed) was removed with filter paper and the samples were weighed on an analytical scale. The method was repeated to constant weight and the WAC was calculated according to Eq. (4) [40].

$$WAC(\%) = \left( \frac{W_h - W_d}{W_d} \right) \times 100 \quad (4)$$

where W<sub>h</sub> is the weight of the hydrated membrane and W<sub>d</sub> is the dry membrane weight.

### 2.14. Water vapor permeance

Water vapor permeance (WVP) was determined gravimetrically according to method E96/96 M-22 [41], according to the standard test method for the transmission of water vapor in materials, with modifications proposed by Carpiné [42]. For this analysis, circular permeation cells made of vinyl polychloride (Poly-(vinyl chloride), 63.5 mm × 58.8 mm, internal diameter × depth) were used, with an exposure area of the films of 0.0028 m<sup>2</sup>. The cells were filled with anhydrous calcium chloride and film samples were placed in the opening of the test cells. The final set was sealed with paraffin and packed in a desiccator containing saturated NaCl solution (25 °C, 75 % ± 5 Relative Humidity). Cell weight gain was monitored every 24 h for 7 days. The analysis was performed in triplicate and the PVA was calculated by Eq. (5).

$$PVA = \frac{G \cdot x}{t \cdot A \cdot S \cdot (R_1 - R_2)} \quad (5)$$

where G/t is the slope of the straight line (g s<sup>-1</sup>); A is the film permeation area (m<sup>2</sup>); x is the thickness in the exposed area of the film (m); S is the saturated steam pressure at test temperature (3169.75 Pa); R<sub>1</sub> is the relative humidity (RH) of the environment containing saturated NaCl solution (75 % RH) expressed in fraction; R<sub>2</sub> is the relative humidity of the environment containing calcium chloride (0 % RH) expressed in a fraction.

### 2.15. Mechanical properties

Dynamic mechanical analyses (DMA) were performed on the DMA Q800 TA Instruments equipment using the membrane tension clamp. Stress-strain tests were performed with a ramp force from 1 N min<sup>-1</sup> to 18 N [43].

### 2.16. Statistical analysis

All measurements were performed with at least three repetitions. The data obtained were presented as mean ± standard deviation. Statistica 7.0 software (StatSoft, Tulsa, Oklahoma, USA) and Origin 7.0 software (OriginLab, Northampton, MA) were used for all statistical analyses.

## 3. Results and discussion

### 3.1. Biosorption behavior

The study of biosorption isotherm was used to characterize extracts and biosorption, presenting the optimal conditions in the kinetic studies. Several models were applied (Supplementary Material, Table S1) to evaluate the biosorption mechanism. Through the parameters found and

the correlation coefficient ( $R^2$ ) it was possible to define the isotherms of the models of two parameters and three parameters that best represented the behavior of the data. The isotherm of Sips ( $R^2$ : 0.9925) and Hills ( $R^2$ : 0.9925) were the ones that best represented the behavior of the data, followed by the isotherms of Redlich-Peterson ( $R^2$ : 0.9863) and Freundlich ( $R^2$ : 0.9814). The Hills model assumes that adsorption is a cooperative phenomenon due to the ability of adsorbate attached to a site to interfere with the binding of this same molecule in a site other than the adsorbent. In contrast, the Sips model combines Langmuir and Freundlich isotherms to predict heterogeneous adsorption systems [44]. This result contradicts Zhang et al. [45], who presented the Langmuir linear equation to accurately describe the adsorption balance ratio in their study of drugs in bacterial cellulose. However, it is important to highlight that each exogenous molecule has a unique character in biosorption behavior in bacterial cellulose. Understandably, kinetic models explain this mechanism of biosorption in different ways.

### 3.2. Phenolic compounds and antioxidant activity of extract and membrane

The extract of the ternary mixture (white tea, hibiscus, and grape pomace) was characterized regarding to the concentration of total phenolic compounds, total flavonoids, and antioxidant activity (Table 3). The literature has presented a concentration of total phenolics for white tea between 726 and 1222.85 mg GAE L<sup>-1</sup> [23,46,47], between 18.98 and 45.98 mg GAE L<sup>-1</sup> for Hibiscus [48,49] and between 37.67 and 1400 mg GAE L<sup>-1</sup> for grape pomace [50,51]. Thus, the concentration of TPC presented in our study for the ternary mixture (871.67 mg GAE L<sup>-1</sup>) agrees with these studies. However, it is essential to highlight that interaction among phenolic compounds can be additive, synergistic, or antagonistic, depending on the classes and the proportion of phenolic compounds from each plant matrix, influencing, therefore, the total phenolic concentration and antioxidant activity of the mixture [52,53].

After biosorption, the extract showed a reduction of TPC (16 %), flavonoids (16 %) and antioxidant activity (38 % for FRAP, 16 % for DPPH, 45 % for ABTS and 60 % TBARS), which evidences that phenolic compounds have probably been transferred to the BC membrane. Additionally, the samples of extracts before and after biosorption showed a significant difference ( $p \leq 0.05$ ).

Phenolic biosorption in BC membrane surface depends on the molecular structure, molar mass and initial concentration of phenolics [27]. As expected, the control membrane had no phenolic compounds or

**Table 3**

Total phenolic compounds (TPC), Total flavonoids (FT) and antioxidant activity of samples.

Analysis	Samples			
	EBB	EAB	BC-Control	BC-Bio
TPC (mg GAE L <sup>-1</sup> )	871.7 <sup>a</sup> ± 4.5	731.6 <sup>b</sup> ± 1.7	ND	64.9 ± 1.4
TF (mg CE L <sup>-1</sup> )	150.9 <sup>a</sup> ± 8.8	126.5 <sup>b</sup> ± 0.8	ND	29.9 ± 1.9
Antioxidant activity	(μmolTE L <sup>-1</sup> )	(μmolTE L <sup>-1</sup> )		(mg g <sup>-1</sup> )
FRAP	2543.5 <sup>a</sup> ± 20.7	1576.8 <sup>b</sup> ± 6.0	ND	130.7 ± 0.5
DPPH	4333.8 <sup>a</sup> ± 3.2	3641.0 <sup>b</sup> ± 6.8	ND	83.4 ± 1.4
ABTS	8147.5 <sup>a</sup> ± 217.5	4480.9 <sup>a</sup> ± 200.1	ND	158.6 ± 32.1
TBARS	380.0 <sup>a</sup> ± 0.9 <sup>1</sup>	150.0 <sup>a</sup> ± 2.7 <sup>1</sup>	ND	234.2 ± 32.2

<sup>ab</sup> Different letters in the same line indicate a statistically significant difference at the 0.05 level by the Tukey test.

<sup>1</sup> Unit in mgTE L<sup>-1</sup>. EBB: extract before biosorption; EAB: extract after biosorption; BC-control: bacterial cellulose control and BC-Bio: bacterial cellulose biosorbed. ND – Not detected. TE: Trolox equivalent.

antioxidant capacity. However, the biosorbed membrane showed a concentration of total phenolics of 64.89 mg L<sup>-1</sup> ± 1.41, which agrees with the other biosorption evidence. This result is similar to Li et al. [5], who obtained a BC with a phenolic compound concentration of 66.09 mg L<sup>-1</sup> ± 2.35 after incorporating the wine residue.

The antioxidant activity of plant extracts is associated with phenolic concentration. The main characteristic is their ability to capture free radicals, thus inhibiting the excessive reactive oxygen species (ROS) that lead to degenerative diseases [54].

The literature shows an affinity between certain compounds with the assay's mechanism of action. For example, the ABTS and DPPH methods act as free radical scavengers, while the FRAP assay is measured by reducing the ferric ion. On the other hand, the TBARS method analyzes the effect of antioxidants on induced lipid peroxidation. Thus, different classes of phenolic compounds in the raw material imply different responses for the methods tested [55].

EBB showed antioxidant activity for all carried-out assays. Because of the biosorption process, EAB showed a reduction varying from 15.98 % (DPPH) to 60.52 % (TBARS), corroborating the idea of phenolic transfer from extracts to BC membrane. Thus, BC-Bio also showed antioxidant activity for tested methods. Similar results of our study were found in the investigation performed by Nowak et al. [6], where BC membrane was incorporated with an extract of *Epilobium angustifolium* L. exhibited a concentration of TPC and antioxidant activity by the DPPH and ABTS methods presented a concentration of 0.63 mmol L<sup>-1</sup>, 1.59 mmolTE L<sup>-1</sup> and 2.09 mmolTE L<sup>-1</sup>, respectively. Therefore, our results corroborate with other researchers where bacterial cellulose membrane was a biomaterial capable of effectively absorbing bioactive compounds with antioxidant capacity. The presence of phenolic compounds in the membrane is positive regarding biological activities since the antioxidant activity is related to antimicrobial activity, healing effect, anti-inflammatory and antiaging [8,27,56].

### 3.3. Identification and quantification of bioactive compounds by chromatography analysis

The chromatographic analysis allowed identifying and quantifying phenolic compounds in extracts and the desorption solution of control and biosorbed bacterial cellulose membranes (Table 4). The results showed a reduction of phenolic acids and flavonoids in extracts after biosorption, corroborating the colorimetric results. This reduction in concentration is expected because it indicates that part of these compounds was biosorbed by the BC membrane. From the sixteen standards used, it is just detected fourteen phenolic compounds in the extracts before and after biosorption was possible. Among phenolic acids, chlorogenic acid (EBB: 40.64 mg L<sup>-1</sup> and EAB: 32.86 mg L<sup>-1</sup>) showed the highest concentration in extracts and flavonoid procyanidin B2 (EBB: 119.86 mg L<sup>-1</sup> and EAB: 70.28 mg L<sup>-1</sup>). It is important to note that grape pomace is rich in procyanidin B2 [57] and Hibiscus has a high concentration of chlorogenic acid [58]. In addition, the presence of ferulic acid, syringic acid, caffeic acid, naringin, isoquercetin, ellagic acid and catechin from *Camellia sinensis* is also highlighted, as well as in the other matrices that make up the extract [57,59].

Colorimetric tests and chromatographic analysis showed the absence of phenolic compounds in the control membrane. However, when subjected to biosorption in an extract with phenolic compounds, it is possible to identify in the desorption solution that the biosorbed membranes present some of these compounds, i.e., procyanidin B2 (2.06 mg L<sup>-1</sup>), vanillic acid (0.51 mg L<sup>-1</sup>), chlorogenic acid (0.28 mg L<sup>-1</sup>), caffeic acid (0.18 mg L<sup>-1</sup>), ferulic acid (0.08 mg L<sup>-1</sup>) and syringic acid (0.07 mg L<sup>-1</sup>). Nowak et al. [6] incorporated the extract of *Epilobium angustifolium* L. in the BC membrane and identified by HPLC the presence of chlorogenic acid (26.78 mg 100 mL<sup>-1</sup>) and caffeic acid (7.13 mg 100 mL<sup>-1</sup>), as well as other compounds common to the extract such as gallic acid, 3,4-dihydroxybenzoic acid, 4-hydroxybenzoic acid and 3-hydroxybenzoic acid. The samples of extracts before and after biosorption

**Table 4**  
Quantification of phenolic compounds in samples.

Phenolic compounds	Samples			
	EBB (mg L <sup>-1</sup> )	EAB (mg L <sup>-1</sup> )	SBCC (mg L <sup>-1</sup> )	SBCB (mg L <sup>-1</sup> )
<b>Phenolic acids</b>				
Gallic acid	0.39 <sup>a</sup> ± 0.03	0.35 <sup>a</sup> ± 0.00	<LOD	<LOD
Chlorogenic acid	40.64 <sup>a</sup> ± 0.16	32.86 <sup>a</sup> ± 1.91	<LOD	0.28 ± 0.01
Vanillic acid	0.74 <sup>a</sup> ± 0.04	0.37 <sup>b</sup> ± 0.02	<LOD	0.51 ± 0.01
Caffeic acid	2.83 <sup>a</sup> ± 0.11	2.47 <sup>a</sup> ± 0.10	<LOD	0.18 ± 0.00
Epicatechin	1.75 <sup>a</sup> ± 0.02	0.46 <sup>b</sup> ± 0.05	<LOD	<LOD
Syringic acid	3.14 <sup>a</sup> ± 0.21	1.89 <sup>b</sup> ± 0.19	<LOD	0.07 ± 0.01
p-Coumaric acid	1.36 <sup>a</sup> ± 0.04	0.80 <sup>b</sup> ± 0.09	<LOD	<LOD
Ferulic acid	4.21 <sup>a</sup> ± 0.19	2.46 <sup>b</sup> ± 0.20	<LOD	0.08 ± 0.01
Naringin	4.59 <sup>a</sup> ± 0.10	4.16 <sup>a</sup> ± 0.07	<LOD	<LOD
<b>Flavonoids</b>				
Isoquercetin	23.15 <sup>a</sup> ± 0.05	18.95 <sup>a</sup> ± 1.15	<LOD	<LOD
Ellagic acid	10.21 <sup>a</sup> ± 0.28	6.54 <sup>b</sup> ± 0.68	<LOD	<LOD
Quercetin	<LOD	<LOD	<LOD	<LOD
Catechin	2.03 <sup>a</sup> ± 0.00	1.44 <sup>b</sup> ± 0.01	<LOD	<LOD
Procyanidin B2	119.86 <sup>a</sup> ± 1.63	70.28 <sup>b</sup> ± 5.36	<LOD	2.06 ± 0.02
Cyanidin-3-glucoside	0.51 <sup>a</sup> ± 0.03	0.19 <sup>b</sup> ± 0.03	<LOD	<LOD

Note: EBB: extract before biosorption; EAB: extract after biosorption; SBCC: solution of BC-Control desorption; SBCB: Solution of BC-biosorbed desorption. LOQ: Limit of quantification; LOD: Limit of detection. <sup>ab</sup> Different letters in the same line indicate a statistically significant difference at the 0.05 level by the Tukey test.

showed significant difference ( $p \leq 0.05$ ) for vanillic, syringic, p-coumaric and ellagic acids as well as quercetin, epicatechin and catechin.

It is noteworthy that the low concentration, compared to the extract after biosorption, may be related to the complete non-desorption of the

compounds in the buffer solution analyzed according to the desorption method. Thus, our results may characterize a delivery system for these compounds. Furthermore, studies have applied a release rate at longer times, between 2 and 26 h, which despite a higher concentration of phenolics, depend on and influence the application of the membrane [5,7].

#### 3.4. Characterization of the chemical structure of the membrane

The grouped spectra of the control and biosorbed membranes are presented in Fig. 1, which describes the peak positions of various functional groups. The MIR-ATR spectra of the biosorbed membrane showed peaks similar to those of the control membrane (666, 1031, 1162, 1109, 1646, 2898 and 3332 cm<sup>-1</sup>). These characteristics of the chemical structure of the bacterial cellulose membrane are in agreement with those presented by Fernandes et al. [19] and Du et al. [60], whose peaks close to 1031 and 1057 refer to the connection of stretching frequencies with those of the curvature of the C-OH groups of carbohydrates (such as glucose and glycogen) [19]. The bands around 3300–3600 cm<sup>-1</sup> are attributed to hydroxide elongation vibration (OH) and its peak (3349 cm<sup>-1</sup>) corresponds to the absorption of the hydrogen bond formed by the hydroxyl group in the bacterial cellulose molecule [61]. Additionally, it is possible to observe that after biosorption, there is only one change in the transmittance of the spectrum bands, with no new absorption peak.

#### 3.5. Identification of membrane characteristics by microscopy

The surface characteristics of the membranes can be observed by micrographs (Fig. 2). It is possible to observe in SEM images that BC-Control (Fig. 2a1 and a2) has more fragile and porous microfibrils than BC-Bio (Fig. 2b1 and b2), which observed compaction of microfibrils after biosorption. This overlap of the layers in BC-Bio is similar to the results observed by Li et al. [5] when adding wine residues in bacterial cellulose biosynthesis. According to Zhou et al. [59], the creation of hydrogen bonds between cellulose and phenolic structures can contribute to crosslinking between polymers and the compaction of membrane structures.

This compaction behavior can be observed on the surfaces of the network structure formed by the membranes analyzed by AFM (Fig. 3), an image size of 3 × 3 μm. It is worth mentioning that during the analysis, a high adhesivity of BC-Control was observed in relation to BC-Bio. In topographic images 3(a) and 3(d), it is possible to observe that

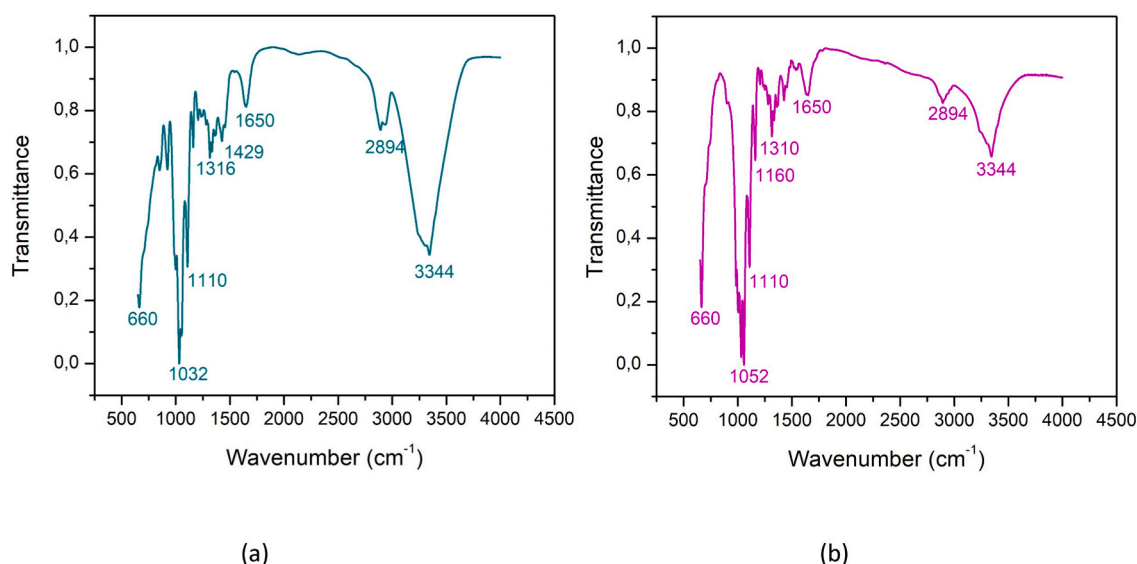


**Fig. 1.** MIR-ATR spectral analysis of BC membranes (a) BC-Control and (b) BC-Bio.

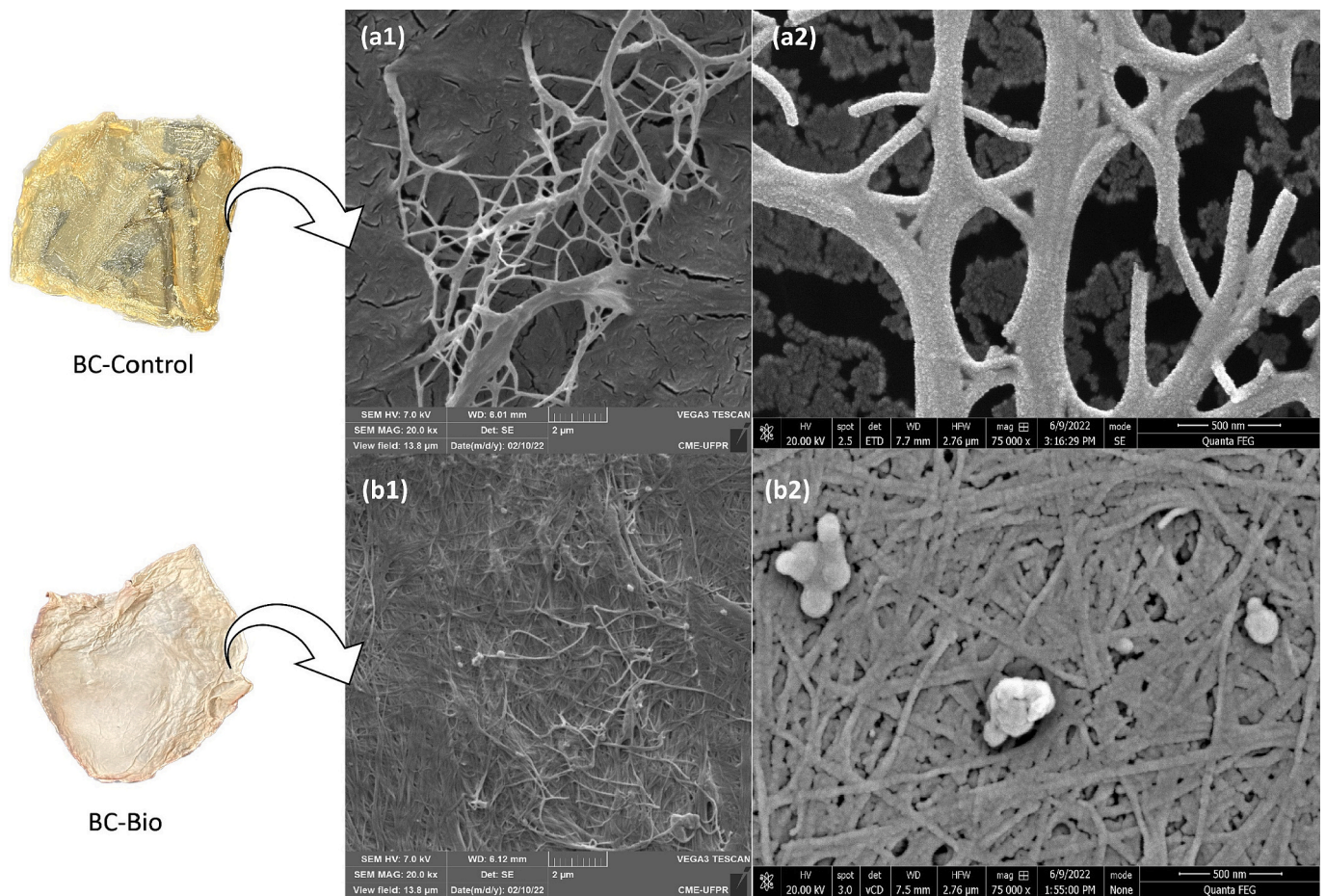


**Fig. 2.** SEM images of the surfaces of the bacterial cellulose (BC) membranes. (a1) BC-Control, magnification 20,000 $\times$ , (b1) BC-Bio, magnification 20,000 $\times$ , (a2) BC-Control, magnification 75,000 $\times$  and (b2) BC-Bio, magnification 75,000 $\times$ .

the structure of the cell wall of membranes contains fibers based on cylindrical cellulose organized in layered structures. Similar microfibrils were observed in the study by Pigaleva et al. [62], in which the structures of cellulose fibrils are well-defined and are individually 50 to 100 nm thick. Furthermore, it was possible to visualize the structures in 2-phase topographic images (Fig. 3(b) and (e)). In Fig. 3(b), it was possible to observe the fibrils and the densest layer of polysaccharides. In Fig. 3e, the fibrils are more compacted, and some points are lighter and brighter. In the 3D-graphs, BC-control (Fig. 3(c)) shows topography with high roughness ( $R_a = 160.47$  nm), while BC-Bio (Fig. 3(f)) shows a decrease in this roughness ( $R_a = 130.38$  nm) after the insertion of phenolic compounds. These results are superior to Wen et al. [3], whose BC membranes present a gentle roughness between 25.8 and 63.4 nm.

### 3.6. Determination of membrane crystallinity

Fig. 4 shows the X-ray diffractograms of the BC-Control and BC-Bio membranes. It was possible to observe that the three peaks presented in BC-Control ( $14.1^\circ$ ,  $16.5^\circ$  and  $22.4^\circ$ ) are like those of BC-Bio ( $14.2^\circ$ ,  $16.4^\circ$  and  $22.4^\circ$ ), differing only in the intensity of these peaks. These peaks represent a typical structure of cellulose I, in agreement with the studies by Liu et al. [61], Zhou et al. [7] and Abrial et al. [63]. The increase in intensity observed in Fig. 4b may be related to how phenolic compounds interact with the membrane in the biosorption process since the increase in the peak diffraction intensity indicates that there were many hydroxy and amino groups in the molecule and that subsequently biosorption there was a new hydrogen bond [61]. The crystalline index of BC-Control and BC-Bio was 22.9 % and 50.35 %, respectively.

Therefore, there was a 55 % increase in membrane crystallinity with the biosorption of phenolic compounds. The high crystallinity corresponds to an internal structure of stable and orderly bacterial cellulose, which results in better mechanical properties of the film [61].

### 3.7. Thermal stability analysis

Two stages of weight loss are displayed in the TG curve of the BC-Control membrane (Fig. 5a) and BC-Bio (Fig. 5b). The first weight loss stage occurs through water evaporation; this process happens more slowly in BC-Bio than in BC-Control. The second stage, which occurs more abruptly, corresponds to the decomposition of cellulose. In this context, it was possible to observe, in the DTG graph, that the thermal stability of the control membrane occurs at the maximum rates of thermal degradation close to  $250^\circ\text{C}$  (Fig. 5B). In comparison, for biosorbed membrane, the degradation occurs at  $350^\circ\text{C}$  (Fig. 5D). Therefore, the biosorption of phenolic compounds has managed to maintain the thermal stability of the membrane, which can withstand thermal degradation up to  $350^\circ\text{C}$ . This increase in thermal stability was also observed in the study by Wen et al. [3], in which the adsorption of anthocyanins of purple potato in BC showed an increase in thermal stability and degradation of cellulose from  $355^\circ\text{C}$ .

### 3.8. Water absorption capacity and water vapor permeability

The BC-Control membrane had a water absorption capacity of  $299.02 \pm 49.56$  %, while BC-Bio had a capacity of  $560.77 \pm 180.97$  %. These values of water absorption capacity are in agreement with the

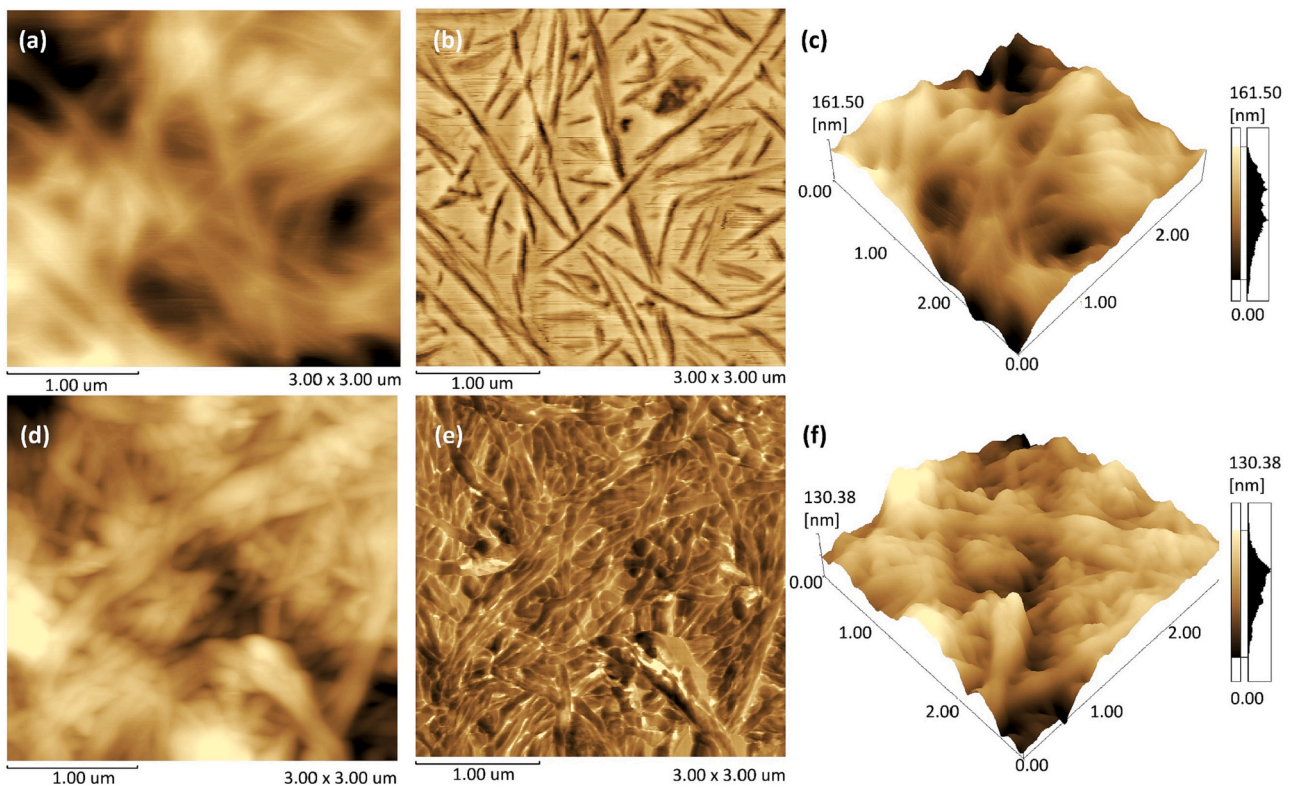


**Fig. 3.** Images  $3 \times 3 \mu\text{m}$  of the surface of the bacterial cellulose membrane. (a) BC-Control topographic image, (b) BC-Control 2-phase topographic image, (c) BC-Control 3D topographic image, (d) BC-Bio topographic image, (e) BC-Bio 2-phase topographic image and (f) BC-Bio 3D topographic image.

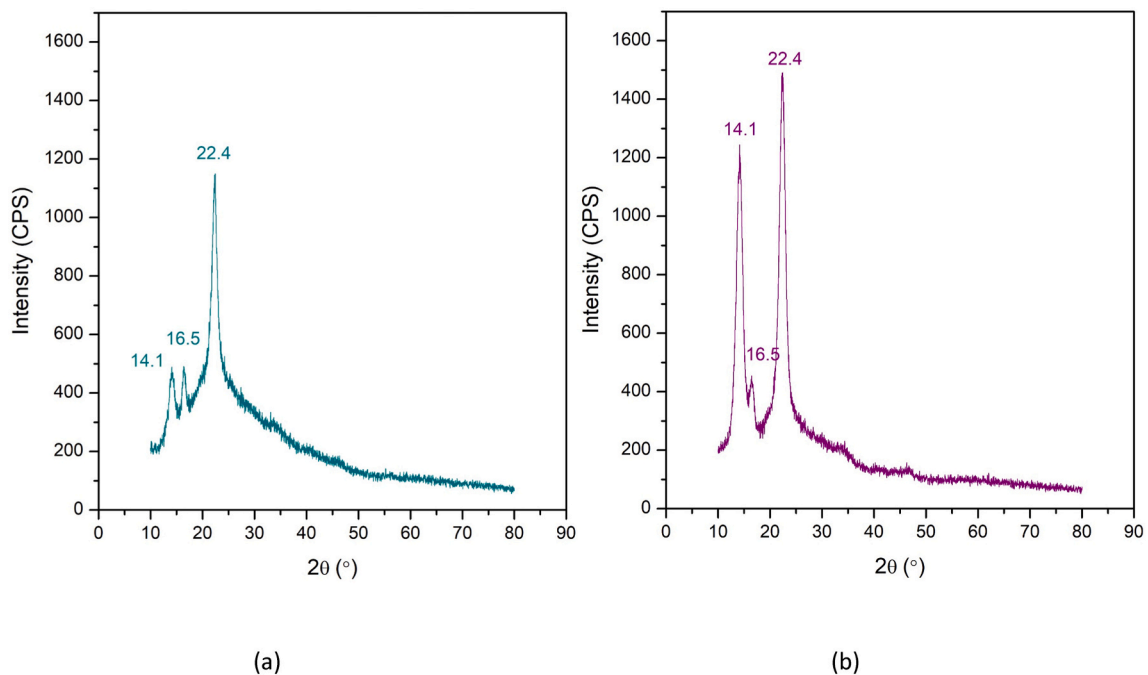


**Fig. 4.** X-ray diffractograms of membranes. (a) BC-Control and (b) BC-Bio.

results presented by Fernandes [38] for bacterial cellulose (365.4–449.9 %) produced in ternary mixture medium (66.7 % white tea, 16.7 % Hibiscus and 16.7 % grape pomace) and statically incubated at  $28^\circ\text{C}$  for ten days. Additionally, it was possible to observe that the water absorption capacity increased by 47 % with the biosorption of phenolic compounds in the membrane. Although pure bacterial cellulose

membranes have a high rehydration capacity, the water contained in the cellulose tape structure is essential in binding phenolic compounds. Thus, due to the positive correlation between the water content and the binding capacity of polyphenols, it was observed that the expansion capacity of cellulose networks contributes to the phenolic-cellulose compound interactions, maintaining the water in its structure and

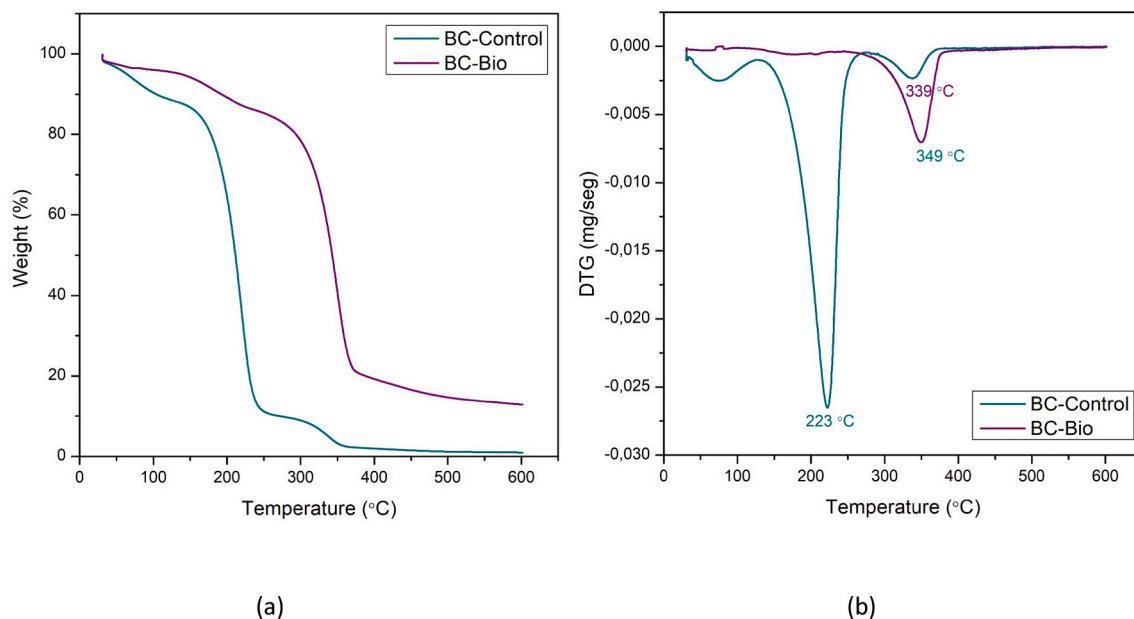


Fig. 5. Thermogravimetric analysis (TG) of bacterial cellulose membrane. (A) Membranes TG, (B) Derived from the TG curve (DTG) of membranes.

increasing its water absorption capacity [26,27]. A high-water absorption capacity is required for an effective bioactive compound delivery system, as this rehydration influences the release rate of these compounds [38].

BC-Control exhibited a water vapor barrier of  $3.51 \times 10^{-6} \text{ g}\cdot\text{m}^{-1}\cdot\text{s}^{-1}\cdot\text{Pa}^{-1}$ . BC-Bio's WVP increased to  $5.15 \times 10^{-6} \text{ g}\cdot\text{m}^{-1}\cdot\text{s}^{-1}\cdot\text{Pa}^{-1}$ , representing a lower water vapor barrier performance. The microfibrils of the bacterial cellulose membrane are well defined, which makes this dense structure makes it difficult to pass water vapor through the membrane. However, compared to the study by Wen et al. [3], the WVP values obtained in our study were higher than those reported for films adsorbed with purple potato anthocyanins ( $3.10$  to  $6.10 \times 10^{-11} \text{ g}\cdot\text{m}^{-1}\cdot\text{s}^{-1}\cdot\text{Pa}^{-1}$ ). In the study by Abiral et al. [63] for bacterial cellulose nanofibers loaded with polyvinyl acid by ultrasonic method, the membrane presented a WVP of  $5.0 \times 10^{-11} \text{ g}\cdot\text{m}^{-1}\cdot\text{s}^{-1}\cdot\text{Pa}^{-1}$ . The low permeability to water vapor represents a suitable property of the water vapor barrier. However, the difference in permeability values may be related to the addition of hydrophobic compounds, which can reduce WVP. Thus, this slows down the diffusion process and decreases the permeability of water vapor [3].

Furthermore, the adhesive bond on the surface, the number of fibers and the better dispersion of the fiber result in obstructions to diffusion, causing the water molecules to walk longer paths between the membrane, thus reducing the permeability of water vapor [63]. This explains the increase in BC-Bio WVP concerning BC-Control since, by AFM analysis, the adhesivity of the same decreased by adding phenolic compounds in the membrane. Therefore, although WVP values are higher than those reported in the literature for other membrane functionalities, the biosorbed membrane still has a barrier to water vapor permeability.

### 3.9. Mechanical properties

The effect of biosorption on the membrane properties of tensile stress, Young's Modulus and elongation at break were evaluated. BC-Control presented a tensile stress property of 33.73 MPa, 6.16 MPa Young's Modulus and 5.47 % elongation at break, while BC-Bio exhibited 70.84 MPa, 10.73 Pa and 0.67 %, respectively. It was possible to observe that after biosorption, there is an increase in the tensile stress parameters (48 %) and the Young's Modulus of the

membrane, as well as a decrease in elongation at break (88 %), resulting in an improvement in the mechanical performance of BC-Bio. This tension-increasing behavior was observed by Rusdi et al. [64] in BC membranes with the addition of Kevlar and epoxy composites, which ranged from 24.59 to 331.38 MPa. Similarly, Aliabadi et al. [43] observed an increase in tension (20–130 MPa) and a decrease in elongation at rupture (1–15 %) when adding tannic acid in micro fibrillated cellulose films (compared to control). These mechanical characteristics, therefore, are promising for bacterial cellulose membranes.

## 4. Conclusions

The biosorption of phenolic compounds from the extract of the ternary mixture (white tea, hibiscus, and grape pomace) in the BC membrane presented the potential for a system of loading and releasing molecules. With the determination of the ideal parameters for the biosorption mechanism and the chemical-mechanical characterization of the membrane, it was observed that the *ex-situ* modification can promote antioxidant activity to BC, as demonstrated by colorimetric and chromatographic tests. Additionally, this *ex-situ* modification can improve the existing properties of the BC membrane, such as increased thermal stability and water absorption capacity, low water vapor permeability and improved mechanical properties. Thus, the PC-BC system can be considered promising for developing innovative technologies in the biomedical (wound dressing, burn dressings and tissue engineering), food (food additive and packaging), pharmaceutical (controlled drug release) and cosmetic areas (face masks, moisturizers, and sunscreens). It is important to highlight that although bacterial cellulose has characteristics of high-water absorption capacity, it may present a low desorption capacity of phenolic compounds, which depend on the interaction forces between PC and BC structures. Thus, knowing how to break these interactions is so important as know how BC membranes adsorb phenolic compounds, optimizing the process for each application of interest.

Supplementary data to this article can be found online at <https://doi.org/10.1016/j.ijbiomac.2023.124349>.

### Declaration of competing interest

The authors declare that they have no known competing financial

interests or personal relationships that could have appeared to influence the work reported in this paper.

## Acknowledgments

The authors would like to thank the National Council for Scientific and Technological Development (CNPq), grant number 304722/2019-7) and Coordination for the Improvement of Higher Education Personnel (CAPES), Contract 88882.381652/2019-01) by funding the research. In addition, the authors would also like to thank the Foundation for Science and Technology (FCT, Portugal) for financial support through national funds FCT/MCTES (PIDDAC) to CIMO (UIDB/00690/2020 and UIDP/00690/2020) and SusTEC (LA/P/0007/2021). National funding by FCT, P.I., through the institutional scientific employment program-contract for L. Barros contract.

## References

- [1] A. Rastogi, R. Banerjee, Statistical optimization of bacterial cellulose production by *Leifsonia soli* and its physico-chemical characterization, *Process Biochem.* 91 (2020) 297–302, <https://doi.org/10.1016/j.procbio.2019.12.021>.
- [2] B.S. Inoue, S. Streit, A.L. dos Santos Schneider, M.M. Meier, Bioactive bacterial cellulose membrane with prolonged release of chlorhexidine for dental medical application, *Int. J. Biol. Macromol.* 148 (2020) 1098–1108, <https://doi.org/10.1016/j.ijbiomac.2020.01.036>.
- [3] Y. Wen, J. Liu, L. Jiang, Z. Zhu, S. He, S. He, W. Shao, Development of intelligent/active food packaging film based on TEMPO-oxidized bacterial cellulose containing thymol and anthocyanin-rich purple potato extract for shelf life extension of shrimp, *Food Packag. Shelf Life* 29 (2021), 100709, <https://doi.org/10.1016/j.fpsl.2021.100709>.
- [4] L.S.F. Leite, C. Pham, S. Bilatto, H.M.C. Azeredo, E.D. Cranston, F.K. Moreira, L.H. C. Mattoso, J. Bras, Effect of tannic acid and cellulose nanocrystals on antioxidant and antimicrobial properties of gelatin films, *ACS Sustain. Chem. Eng.* 9 (2021) 8539–8549, <https://doi.org/10.1021/acsschemeng.1c01774>.
- [5] Z. Li, F. Azi, J. Dong, L. Liu, Z. Ge, M. Dong, Green and efficient in-situ biosynthesis of antioxidant and antibacterial bacterial cellulose using wine pomace, *Int. J. Biol. Macromol.* 193 (2021) 2183–2191, <https://doi.org/10.1016/j.ijbiomac.2021.11.049>.
- [6] A. Nowak, P. Ossowicz-Rupniewska, R. Rakoczy, M. Konopacki, M. Peruzińska, M. Drozdziak, E. Makuch, W. Duchnik, L. Kucharski, K. Wenelska, A. Klimowicz, Bacterial cellulose membrane containing *Epilobium angustifolium* L. extract as a promising material for the topical delivery of antioxidants to the skin, *Int. J. Mol. Sci.* 22 (2021) 6269, <https://doi.org/10.3390/ijms22126269>.
- [7] X. Zhou, X. Liu, Q. Wang, G. Lin, H. Yang, D. Yu, S.W. Cui, W. Xia, Antimicrobial and antioxidant films formed by bacterial cellulose, chitosan and tea polyphenol – shelf life extension of grass carp, *Food Packag. Shelf Life* 33 (2022), 100866, <https://doi.org/10.1016/j.fpsl.2022.100866>.
- [8] A.C. Pedro, O.G. Paniz, I. de A.A. Fernandes, D.G. Bortolini, F.T.V. Rubio, C.W. I. Haminiuk, G.M. Maciel, W.L.E. Magalhães, The importance of antioxidant biomaterials in human health and technological innovation: a review, *Antioxidants* 11 (2022) 1644, <https://doi.org/10.3390/antiox11091644>.
- [9] A. Najafpour, A. Rajabi Khorrami, P. Aberoomand Azar, M. Saber Tehrani, Study of heavy metals biosorption by tea fungus in kombucha drink using Central Composite Design, *J. Food Compos. Anal.* 86 (2020), 103359, <https://doi.org/10.1016/j.jfca.2019.103359>.
- [10] W.V. Maroldi, G.M. Maciel, R. Rossetto, D.G. Bortolini, I. de A.A. Fernandes, C.W. I. Haminiuk, Biosorption of phenolic compounds from *Plinia cauliflora* seeds in residual yeast: kinetic, equilibrium, and bioaccessibility studies, *Food Process. Preserv.* (2022), <https://doi.org/10.1111/jfpp.17156>.
- [11] R. Rossetto, G.M. Maciel, I. de A.A. Fernandes, T.A. Modkovski, M.A. Semião, T. Brugnari, C.W.I. Haminiuk, Açai seeds as a prospective biosorbent for acid dyes removal, *Chem. Biochem. Eng. Q.* (2022), <https://doi.org/10.15255/CABEQ.2021.1979>.
- [12] A.A. Beni, A. Esmaili, Biosorption, an efficient method for removing heavy metals from industrial effluents: a review, *Environ. Technol. Innov.* 17 (2020), 100503, <https://doi.org/10.1016/j.eti.2019.100503>.
- [13] V.R. Ribeiro, I. de A.A. Fernandes, I.P. Mari, A.P. Stafussa, R. Rossetto, G. M. Maciel, C.W.I. Haminiuk, Bringing together *Saccharomyces cerevisiae* and bioactive compounds from plants: a new function for a well-known biosorbent, *J. Funct. Foods* 60 (2019), 103433, <https://doi.org/10.1016/j.jff.2019.103433>.
- [14] L. Chen, C. Gnanaraj, P. Arulselvan, H. El-Seedi, H. Teng, A review on advanced microencapsulation technology to enhance bioavailability of phenolic compounds: based on its activity in the treatment of type 2 diabetes, *Trends Food Sci. Technol.* 85 (2019) 149–162, <https://doi.org/10.1016/j.tifs.2018.11.026>.
- [15] D.G. Bortolini, C.V. Haminiuk, A.C. Pedro, I. de A.A. Fernandes, G.M. Maciel, Processing, chemical signature and food industry applications of *Camellia sinensis* teas: an overview, *Food Chem.: X* 12 (2021), 100160, <https://doi.org/10.1016/j.fochx.2021.100160>.
- [16] E.T. Albergaria, A.F.M. Oliveira, U.P. Albuquerque, The effect of water deficit stress on the composition of phenolic compounds in medicinal plants, *S. Afr. J. Bot.* 131 (2020) 12–17, <https://doi.org/10.1016/j.sajb.2020.02.002>.
- [17] D.G. Bortolini, G.M. Maciel, I. de A.A. Fernandes, R. Rossetto, T. Brugnari, V. R. Ribeiro, C.W.I. Haminiuk, Biological potential and technological applications of red fruits: an overview, *Food Chem. Adv.* 1 (2022), 100014, <https://doi.org/10.1016/j.focha.2022.100014>.
- [18] I. de A.A. Fernandes, G.M. Maciel, W.V. Maroldi, D.G. Bortolini, A.C. Pedro, C.W. I. Haminiuk, Bioactive compounds, health-promotion properties and technological applications of Jabuticaba: a literature overview, *Measurement: Food* 8 (2022), 100057, <https://doi.org/10.1016/j.meafoo.2022.100057>.
- [19] I. de A.A. Fernandes, G.M. Maciel, A.L.M.S. Oliveira, A.J.F. Miorim, J.D. Fontana, V.R. Ribeiro, C.W.I. Haminiuk, Hybrid bacterial cellulose-collagen membranes production in culture media enriched with antioxidant compounds from plant extracts, *Polym. Eng. Sci.* 60 (2020) 2814–2826, <https://doi.org/10.1002/pen.25514>.
- [20] T.R. Dias, M.G. Alves, G.D. Tomás, S. Socorro, B.M. Silva, P.F. Oliveira, White tea as a promising antioxidant medium additive for sperm storage at room temperature: a comparative study with green tea, *J. Agric. Food Chem.* 62 (2014) 608–617, <https://doi.org/10.1021/jf4049462>.
- [21] T.R. Dias, D.F. Carrageta, M.G. Alves, P.F. Oliveira, B.M. Silva, White tea, in: *Nonvitamin And Nonmineral Nutritional Supplements*, Elsevier, 2019, pp. 437–445, <https://doi.org/10.1016/B978-0-12-812491-8.00058-8>.
- [22] G. Riaz, R. Chopra, A review on phytochemistry and therapeutic uses of *Hibiscus sabdariffa* L, *Biomed. Pharmacother.* 102 (2018) 575–586, <https://doi.org/10.1016/j.biopha.2018.03.023>.
- [23] S. Pérez-Burillo, R. Giménez, J.A. Rufián-Henares, S. Pastoriza, Effect of brewing time and temperature on antioxidant capacity and phenols of white tea: relationship with sensory properties, *Food Chem.* 248 (2018) 111–118, <https://doi.org/10.1016/j.foodchem.2017.12.056>.
- [24] M. Gómez-Brandón, M. Lores, H. Insam, J. Domínguez, Strategies for recycling and valorization of grape marc, *Crit. Rev. Biotechnol.* 39 (2019) 437–450, <https://doi.org/10.1080/07388551.2018.1555514>.
- [25] S. Hestrin, M. Schramm, Synthesis of cellulose by *Acetobacter xylinum*, *Biochem. J.* 58 (1954) 345–352, <https://doi.org/10.1042/bj0580337>.
- [26] M. Liu, S. Li, Y. Xie, S. Jia, Y. Hou, Y. Zou, C. Zhong, Enhanced bacterial cellulose production by *Glucanacetobacter xylinus* via expression of *Vitreoscilla hemoglobin* and oxygen tension regulation, *Appl. Microbiol. Biotechnol.* 102 (2018) 1155–1165, <https://doi.org/10.1007/s00253-017-8680-z>.
- [27] I. de A.A. Fernandes, G.M. Maciel, V.R. Ribeiro, R. Rossetto, A.C. Pedro, C.W. I. Haminiuk, The role of bacterial cellulose loaded with plant phenolics in prevention of UV-induced skin damage, *Carbohydr. Polym. Technol. Applic.* 2 (2021), 100122, <https://doi.org/10.1016/j.carpta.2021.100122>.
- [28] V.R. Ribeiro, G.M. Maciel, M.M. Fachi, R. Pontarolo, I. de A.A. Fernandes, A. P. Stafussa, C.W.I. Haminiuk, Improvement of phenolic compound bioaccessibility from yerba mate (*Ilex paraguariensis*) extracts after biosorption on *Saccharomyces cerevisiae*, *Food Res. Int.* 126 (2019), 108623, <https://doi.org/10.1016/j.foodres.2019.108623>.
- [29] N. Ayawei, A.N. Ebelegi, D. Wankasi, Modelling and interpretation of adsorption isotherms, *J. Chem.* 2017 (2017) 1–11, <https://doi.org/10.1155/2017/3039817>.
- [30] S. Rangabhashiyam, N. Anu, M.S. Giri Nandagopal, N. Selvaraju, Relevance of isotherm models in biosorption of pollutants by agricultural byproducts, *J. Environ. Chem. Eng.* 2 (2014) 398–414, <https://doi.org/10.1016/j.jece.2014.01.014>.
- [31] W. Yang, E. Fortunati, F. Dominici, G. Giovanale, A. Mazzaglia, G.M. Balestra, J. M. Kenny, D. Puglia, Effect of cellulose and lignin on disintegration, antimicrobial and antioxidant properties of PLA active films, *Int. J. Biol. Macromol.* 89 (2016) 360–368, <https://doi.org/10.1016/j.ijbiomac.2016.04.068>.
- [32] V.L. Singleton, J.A. Rossi, Colorimetry of total phenolics with phosphomolybdic-phosphotungstic acid reagents, *Am. J. Enol. Vitic.* 16 (1965) 144.
- [33] W. Brand-Williams, M.E. Cuvelier, C. Berset, Use of a free radical method to evaluate antioxidant activity, *LWT Food Sci. Technol.* 28 (1995) 25–30, [https://doi.org/10.1016/S0023-6438\(95\)80008-5](https://doi.org/10.1016/S0023-6438(95)80008-5).
- [34] R. Re, N. Pellegrini, A. Proteggente, A. Pannala, M. Yang, C. Rice-Evans, Antioxidant activity applying an improved ABTS radical cation decolorization assay, *Free Radic. Biol. Med.* 26 (1999) 1231–1237, [https://doi.org/10.1016/S0891-5849\(98\)00315-3](https://doi.org/10.1016/S0891-5849(98)00315-3).
- [35] I.F.F. Benzie, J.J. Strain, The ferric reducing ability of plasma (FRAP) as a measure of “antioxidant power”: the FRAP assay, *Anal. Biochem.* 239 (1996) 70–76, <https://doi.org/10.1006/abio.1996.0292>.
- [36] J. Pinela, L. Barros, M. Duenas, A.M. Carvalho, C. Santos-Buelga, I.C.F.R. Ferreira, Antioxidant activity, ascorbic acid, phenolic compounds and sugars of wild and commercial *Tuberaria lignosa* samples: effects of drying and oral preparation methods, *Food Chem.* 135 (2012) 1028–1035, <https://doi.org/10.1016/j.foodchem.2012.05.038>.
- [37] D.R. Ruka, G.P. Simon, K.M. Dean, Altering the growth conditions of *Glucanacetobacter xylinus* to maximize the yield of bacterial cellulose, *Carbohydr. Polym.* 89 (2012) 613–622, <https://doi.org/10.1016/j.carbpol.2012.03.059>.
- [38] I. de A.A. Fernandes, Desenvolvimento de biofilme de celulose bacteriana enriquecido com compostos bioativos de origem vegetal e colágeno hidrolisado, Mestrado em Engenharia de Alimentos, Universidade Federal do Paraná, 2019. <https://hdl.handle.net/1884/59981>.
- [39] L. Dehabadi, A.H. Karoyo, L.D. Wilson, Spectroscopic and thermodynamic study of biopolymer adsorption phenomena in heterogeneous solid-liquid systems, *ACS Omega* 3 (2018) 15370–15379, <https://doi.org/10.1021/acsomega.8b01663>.
- [40] O. Saibuatong, M. Phisalaphong, *Novo aloe vera*–bacterial cellulose composite film from biosynthesis, *Carbohydr. Polym.* 79 (2010) 455–460, <https://doi.org/10.1016/j.carbpol.2009.08.039>.

- [41] ASTM, Test Methods for Gravimetric Determination of Water Vapor Transmission Rate of Materials, ASTM International, West Conshohocken, 2022, [https://doi.org/10.1520/E0096\\_E0096M-22](https://doi.org/10.1520/E0096_E0096M-22).
- [42] D. Carpiné, Desenvolvimento e caracterização de filme emulsionado biodegradável produzido a partir de proteína isolada de soja, óleo de coco e surfactantes naturais, Doutorado em Engenharia de Alimentos, Universidade Federal do Paraná, 2015.
- [43] M. Aliabadi, B.S. Chee, M. Matos, Y.J. Cortese, M.J.D. Nugent, T.A.M. de Lima, W. L.E. Magalhães, G.G. de Lima, M.D. Firouzabadi, Microfibrillated cellulose films containing chitosan and tannic acid for wound healing applications, *J. Mater. Sci. Mater. Med.* 32 (2021) 67, <https://doi.org/10.1007/s10856-021-06536-4>.
- [44] A.M.D. Canteli, Adsorção de corante por um biossorbente obtido do casulo do bicho-da-seda (*Bombyx mori*): experimentos e modelagem, Doutorado em Engenharia de Alimentos, Universidade Federal do Paraná, 2018.
- [45] W. Zhang, X. Wang, J. Wang, L. Zhang, Drugs adsorption and release behavior of collagen/bacterial cellulose porous microspheres, *Int. J. Biol. Macromol.* 140 (2019) 196–205, <https://doi.org/10.1016/j.ijbiomac.2019.08.139>.
- [46] E. Damiani, T. Bacchetti, L. Padella, L. Tiano, P. Carloni, Antioxidant activity of different white teas: comparison of hot and cold tea infusions, *J. Food Compos. Anal.* 33 (2014) 59–66, <https://doi.org/10.1016/j.jfca.2013.09.010>.
- [47] E. Venditti, T. Bacchetti, L. Tiano, P. Carloni, L. Greci, E. Damiani, Hot vs. cold water steeping of different teas: do they affect antioxidant activity? *Food Chem.* 119 (2010) 1597–1604, <https://doi.org/10.1016/j.foodchem.2009.09.049>.
- [48] Y.W. Mak, L.O. Chuah, R. Ahmad, R. Bhat, Antioxidant and antibacterial activities of hibiscus (*Hibiscus rosa-sinensis* L.) and Cassia (*Senna bicapsularis* L.) flower extracts, *J. King Saud Univ. Sci.* 25 (2013) 275–282, <https://doi.org/10.1016/j.jksus.2012.12.003>.
- [49] J. Zhen, T.S. Villani, Y. Guo, Y. Qi, K. Chin, M.-H. Pan, C.-T. Ho, J.E. Simon, Q. Wu, Phytochemistry, antioxidant capacity, total phenolic content and anti-inflammatory activity of *Hibiscus sabdariffa* leaves, *Food Chem.* 190 (2016) 673–680, <https://doi.org/10.1016/j.foodchem.2015.06.006>.
- [50] C. Negro, L. Tommasi, A. Miceli, Phenolic compounds and antioxidant activity from red grape marc extracts, *Bioresour. Technol.* 87 (2003) 41–44, [https://doi.org/10.1016/S0960-8524\(02\)00202-X](https://doi.org/10.1016/S0960-8524(02)00202-X).
- [51] F.T.V. Rubio, G.M. Maciel, M.V. da Silva, V.G. Corrêa, R.M. Peralta, C.W. I. Haminiuk, Enrichment of waste yeast with bioactive compounds from grape pomace as an innovative and emerging technology: kinetics, isotherms and bioaccessibility, *Innovative Food Sci. Emerg. Technol.* 45 (2018) 18–28, <https://doi.org/10.1016/j.ifset.2017.09.004>.
- [52] J. Enko, A. Gliszczynska-Świągło, Influence of the interactions between tea (*Camellia sinensis*) extracts and ascorbic acid on their antioxidant activity: analysis with interaction indexes and isobolograms, *Food Addit. Contam. A* 32 (2015) 1234–1242, <https://doi.org/10.1080/19440049.2015.1049218>.
- [53] D. Skroza, I. Generalić Mekinić, S. Svilović, V. Šimat, V. Katalinić, Investigation of the potential synergistic effect of resveratrol with other phenolic compounds: a case of binary phenolic mixtures, *J. Food Compos. Anal.* 38 (2015) 13–18, <https://doi.org/10.1016/j.jfca.2014.06.013>.
- [54] B. Mahdi-Pour, S.L. Jothy, L.Y. Latha, Y. Chen, S. Sasidharan, Antioxidant activity of methanol extracts of different parts of *Lantana camara*, *Asian Pac. J. Trop. Biomed.* 2 (2012) 960–965, [https://doi.org/10.1016/S2221-1691\(13\)60007-6](https://doi.org/10.1016/S2221-1691(13)60007-6).
- [55] R. Apak, K. Güçlü, B. Demirata, M. Özyürek, S. Çelik, B. Bektaşoğlu, K. Berker, D. Özyurt, Comparative evaluation of various total antioxidant capacity assays applied to phenolic compounds with the CUPRAC assay, *Molecules* 12 (2007) 1496–1547, <https://doi.org/10.3390/12071496>.
- [56] I. de A.A. Fernandes, A.C. Pedro, V.R. Ribeiro, D.G. Bortolini, M.S.C. Ozaki, G. M. Maciel, C.W.I. Haminiuk, Bacterial cellulose: from production optimization to new applications, *Int. J. Biol. Macromol.* 164 (2020) 2598–2611, <https://doi.org/10.1016/j.ijbiomac.2020.07.255>.
- [57] K.I.B. Moro, A.B.B. Bender, D. de F. Ferreira, C.S. Speroni, J.S. Barin, L.P. da Silva, N.G. Penna, Recovery of phenolic compounds from grape pomace (*Vitis vinifera* L.) by microwave hydrodiffusion and gravity, *LWT* 150 (2021), 112066, <https://doi.org/10.1016/j.lwt.2021.112066>.
- [58] H.-W. Mok, M.-J. Ko, H.-J. Choi, M.-S. Chung, Extraction of chlorogenic acids from hibiscus (*Hibiscus syriacus* L.) by subcritical-water, *J. Ind. Eng. Chem.* 111 (2022) 255–262, <https://doi.org/10.1016/j.jiec.2022.04.005>.
- [59] B. Zhou, Z. Wang, P. Yin, B. Ma, C. Ma, C. Xu, J. Wang, Z. Wang, D. Yin, T. Xia, Impact of prolonged withering on phenolic compounds and antioxidant capability in white tea using LC-MS-based metabolomics and HPLC analysis: comparison with green tea, *Food Chem.* 368 (2022), 130855, <https://doi.org/10.1016/j.foodchem.2021.130855>.
- [60] R. Du, F. Zhao, Q. Peng, Z. Zhou, Y. Han, Production and characterization of bacterial cellulose produced by *Gluconacetobacter xylinus* isolated from Chinese persimmon vinegar, *Carbohydr. Polym.* 194 (2018) 200–207, <https://doi.org/10.1016/j.carbpol.2018.04.041>.
- [61] X. Liu, Y. Xu, C. Guo, C. Zhang, S. Liu, J. Gao, G. Lin, H. Yang, W. Xia, Effect of chitosan grafting oxidized bacterial cellulose on dispersion stability and modulability of biodegradable films, *Int. J. Biol. Macromol.* 204 (2022) 510–519, <https://doi.org/10.1016/j.ijbiomac.2022.02.004>.
- [62] M.A. Pigaleva, M.V. Bulat, T.I. Gromovkyh, I.A. Gavryushina, S.V. Lutsenko, M. O. Gallyamov, I.V. Novikov, A.G. Buyanovskaya, O.I. Kiselyova, A new approach to purification of bacterial cellulose membranes: what happens to bacteria in supercritical media? *J. Supercrit. Fluids* 147 (2019) 59–69, <https://doi.org/10.1016/j.supflu.2019.02.009>.
- [63] H. Abiral, Kadriadi, M. Mahardika, D. Handayani, E. Sugiarti, A.N. Muslimin, Characterization of disintegrated bacterial cellulose nanofibers/PVA bionanocomposites prepared via ultrasonication, *Int. J. Biol. Macromol.* 135 (2019) 591–599, <https://doi.org/10.1016/j.ijbiomac.2019.05.178>.
- [64] R.A.A. Rusdi, N.A. Halim, N.M. Nurazzi, Z.H.Z. Abidin, N. Abdullah, F.C. Ros, N. Ahmad, A.F.M. Azmi, The effect of layering structures on mechanical and thermal properties of hybrid bacterial cellulose/Kevlar reinforced epoxy composites, *Heliyon* 8 (2022), e09442, <https://doi.org/10.1016/j.heliyon.2022.e09442>.